

An Equation of State for Hard Convex Body Chains

Richard J. Sadus

Computer Simulation and Physical Applications Group

School of Information Technology

Swinburne University of Technology

PO Box 218 Hawthorn

Victoria 3122

Australia

email: RSadus@swin.edu.au

Published in: *Molecular Physics* **97**, 1279-1284 (1999).

Abstract

The thermodynamic perturbation theory of hard-sphere chains is generalised to derive an equation of state for hard convex body chains. The hard convex body chain equation of state contains two parameters that are related directly and rigorously to the geometry of the hard convex body. The compressibility factors and second virial coefficients of chains composed of prolate spherocylinders, oblate spherocylinders and doublecones are calculated and compared with hard-sphere chain calculations. The comparison indicates that the nature of the hard convex body has a profound influence on the properties of the chain.

1. Introduction

The concept of hard-sphere repulsion has proved very useful in modelling the intermolecular repulsion of real fluids [1]. Accurate hard-sphere terms such as those proposed by Carnahan and Starling [2] and Guggenheim [3] have been incorporated into many useful equations of state. Indeed, the Carnahan-Starling hard-sphere term is at the heart of most theoretically-based equations of state [4]. Most commonly used equations of state were designed initially for relatively simple molecules but progress [4] is being made increasingly on the accurate description of the properties of large, complicated molecules. The hard-sphere concept has also proved very useful in modelling chain molecules. Typically, a molecular chain can be modelled as a collection of tangent hard-spheres. Chiew [5] developed a rigorous method for representing chains of hard-spheres that has been formulated [6] into a useful equation of state for polymers. Wertheim [7] proposed a thermodynamic perturbation theory (TPT) that is the theoretical basis of the statistical associating fluid theory (SAFT) [8] for real molecules. Ghonasgi and Chapman [9], Chang and Sandler [10] and Sadus [11, 12] improved the accuracy of TPT-type equations by including contributions from dimer interactions.

Despite the usefulness of the hard-sphere concept, most real molecules are neither spherical nor spherically symmetric. To account for the non-spherical geometries of real molecules, the hard-sphere equations of state are often modified to include the effects of anisotropy. For example, equations of state such as the simplified perturbed hard-chain theory equation of state (SPHCT) [13] specifically include an anisotropic parameter. A theoretically rigorous approach to account for non-spherical geometry has been reported by Boublík [14] who used Kihara's [15] concept of a hard convex body (HCB) as the basis of an equation of state for hard non-spherical bodies. The HCB concept has been used successfully [16-18] to predict the properties of simple polyatomic fluids and it forms part of the BACK [19] equation of state. Recently, Pfohl and Brunner [20] modified SAFT [8] by using the BACK [19] equation of state. However, the HCB concept has not been used as the primary representation for molecular chains of non-spherical constituents.

In general, a chain of hard convex bodies is likely to be a better representation of the geometry of many real chain molecules than the hard-sphere chain. Therefore, the properties calculated for the HCB chain are more likely to reflect accurately the actual properties of the molecular fluid. The aim of this work is to formulate a hard convex body chain equation of state which is capable of representing the properties of molecular chains composed of non-spherical segments.

2. Theory

The starting point for our derivation of a hard convex body equation of state to consider the generalisation of Wertheim's TPT model as described by Chapman et al. [21] which relates the compressibility factor of the hard-sphere chain (Z_{HSC}) to the compressibility factor of m hard-spheres (Z_{HS}) via:

$$Z_{HSC} = mZ_{HS} - (m-1) \left(1 + \eta \frac{\partial \ln g_{HS}(\sigma)}{\partial \eta} \right) \quad (1)$$

where $g_{HS}(\sigma)$ is the hard-sphere site-site correlation function at contact, σ is the hard-sphere diameter, $\eta = \pi m \rho \sigma^3 / 6$ is the packing fraction, and ρ is the number density. Although more accurate hard-sphere chains have been developed [9-12], they typically involve contributions from dimer properties. Comparison [11] with molecular simulation data and alternative equations of state indicates that eq. (1) is reasonably accurate for chains of moderate size.

We propose that the compressibility factor (Z_{HCBC}) of a chain composed of m hard convex bodies can be obtained from the hard convex body compressibility factor (Z_{HCB}) and the hard convex body site-site correlation function at contact ($g_{HCB}(\sigma)$) via the following equation which is analogous to eq. (1).

$$Z_{HCBC} = mZ_{HCB} - (m-1) \left(1 + \eta \frac{\partial \ln g_{HCB}(\sigma)}{\partial \eta} \right) \quad (2)$$

To formulate eq. (2) into an explicit equation of state, we require formulae for both the compressibility factor and site-site correlation function at contact of hard convex bodies. The HCB compressibility factor can be obtained accurately from [14]:

$$Z_{HCB} = \frac{1 + (3\alpha - 2)\eta + (3\alpha^2 - 3\alpha + 1)\eta^2 - \alpha^2\eta^3}{(1 - \eta)^3} \quad (3)$$

In eq. (3), α is the deviation from non-spherical geometry which is obtained by considering the mean radius (R), surface area (S) and volume (V) of one convex body:

$$\alpha = \frac{RS}{3V} \quad (4)$$

In the limiting case of a hard-sphere, $\alpha = 1$, and eq. (3) becomes identical to the Carnahan-Starling [2] equation. The site-site correlation function at contact for hard convex bodies is given by [22]:

$$g_{HCB} = 1 + S_R \left(\frac{1 - \eta/2}{(1 - \eta)^3} - 1 \right) \quad (5)$$

In eq. (5), S_R is the ratio of the actual surface area of the HCB (S_{HCB}) to the surface area of hard-spheres ($S_{HS}(equiv)$) occupying a diameter equivalent to the HCB diameter:

$$S_R = \frac{S_{HCB}}{S_{HS}(equiv)} \quad (6)$$

Expressions for S_R required in this work are summarised in Table 1. To obtain S_R , first the equivalent hard-sphere diameter (d_{eq}) is found by equating the expression for the volume of a hard-sphere with the formula for the volume of the HCB. The equivalent hard-sphere surface area (πd_{eq}^2) can be evaluated from d_{eq} which, in addition to the formula for S_{HCB} , permits the evaluation of eq. (6). In the limiting case when $S_R = 1$, eq. (5) becomes the well-known Percus-Yevick [23] equation for the site-site correlation function at contact of hard-spheres.

Inserting, eqs (5) and (3) into eq. (2) and evaluating the derivative of the logarithm of the HCB site-site correlation function at contact with respect to the packing fraction, we obtain:

$$Z_{HCB} = \frac{m(1 + (3a - 2)h + (3a^2 - 3a + 1)h^2 - a^2h^3)}{(1 - h)^3} - (m - 1) \left(1 + \frac{2.5S_R h - S_R h^2}{(1 - h)(1 - (3 - 2.5S_R)h + (3 - 3S_R)h^2 - (1 - S_R)h^3)} \right) \quad (7)$$

In general, the second virial coefficient (B_2) can be obtained from the compressibility factor by applying the thermodynamic relationship [24]:

$$B_2 = \left(\frac{\partial Z}{\partial \rho} \right)_{\rho=0} \quad (8)$$

Applying eq. (8), to eq.(7), we find that the reduced second virial coefficient of the hard convex body chain is:

$$B^* = \frac{B_2}{m^2 \mathbf{S}^3} = \frac{P}{6} \left(3\mathbf{a} + 1 - 2.5S_R + \frac{2.5S_R}{m} \right) \quad (9)$$

An interesting consequence of eq. (9) is that it indicates that under some circumstances, the second virial coefficient of a hard convex body chain can have a negative value. As α , m and S_R can only take positive values, the second virial coefficient can only be negative when $m > 1$ and:

$$S_R > \frac{3\alpha + 1}{2.5(1 - 1/m)} \quad (10)$$

3. Results and Discussion

To examine the effect of molecular shape on the compressibility factor and the second virial coefficient, we have studied chains consisting of spheres, prolate spherocylinders, oblate spherocylinders and doublecones. These shapes were chosen because they reflect the overall geometry of many real molecules. The spherocylinders and doublecone also represent significant departures from spherical geometry. The geometrically dependent properties of these shapes such as mean curvature, surface area and volume depend on their breadth to width ratio (γ). The formulae for several different shapes have been given by Boublík and Nezbeda [25]. The relationships for the HCB geometries used in this work are summarised in Table 1. The dependence of molecular geometry on γ means that the non-sphericity parameter, α , is a function of γ . The formulae for α in terms of γ are summarised in Table 1. In the case of hard-spheres, $\alpha = \gamma = 1$.

The compressibility factor calculated from the HCB-chain equation of state (eq.(7)) as a function of packing fraction for chains consisting of prolate spherocylinder, oblate spherocylinders and doublecone segments are illustrated in Figures 1,2 and, 3 respectively. Irrespective of the shape of the HCB segment, the calculations of the compressibility factor reported here are for chain lengths of 100σ . The 100σ chains are composed of m hard-spheres, m prolate spherocylinders, m oblate spherocylinders or m doublecones. The breadth of all the HCBs is σ and therefore, $\gamma = 100/m$. In

each case, a comparison is presented for chains with different m HCB segments and the all hard-sphere chain.

Comparing the data in Figures 1-3 with each other indicates that, at any packing fraction, the compressibility factor of doublecone chains (Figure 3) is considerably greater than prolate spherocylinder chains (Figure 1) which in turn is greater than the compressibility factor of oblate spherocylinders (Figure 2). At low packing fractions ($\eta < 0.15$), the compressibility factor of the various chains is similar irrespective of the shape of the HCB segment. However, at moderate to high packing fractions ($\eta > 0.3$), the shape of the HCB has a considerable effect on the observed compressibility factor.

The compressibility factor is also very sensitive to the number of HCB segments in the chain. Initially as the number of HCBs in the chain is increased (i.e., increased m), the compressibility factor is lowered substantially. This may reflect the greater conformational flexibility of a multi-segment chain. However, if m is increased further, the reduction in the compressibility factor is halted and the compressibility factor begins to increase and approach the hard-sphere chain value. This changeover point is different for the different HCB chains. For either prolate spherocylinder (Figure 1) or oblate spherocylinder chains (Figure 2) it occurs for $m > 30$, whereas for doublecone chains (Figure 3), the changeover occurs for $m > 50$.

It is also interesting to observe when the compressibility factor of the HCB chains becomes less than the compressibility factor of the all hard-sphere chain. The number of segments required to achieve this depends clearly on the nature of the HCB. For the oblate spherocylinder chains it occurs when $m = 5$ (Figure 2) whereas at least 10 segments are required for the prolate spherocylinder (Figure 3). In the vicinity of 50 doublecone segments (Figure 3) are required to reduce the compressibility factor below the all hard-sphere value.

The reduced second virial coefficient of the different HCB chains of varying chain length (from 5σ to 100σ) as a function of number of segments is illustrated in Figures 4-6. It is apparent from the data in these figures that the reduced second virial coefficient for doublecone chains (Figure 6) is considerably larger than for prolate spherocylinders (Figure 4) which in turn have larger values than oblate spherocylinder chains (Figure 5). Irrespective, of the nature of the HCB segment, the second virial coefficient declines progressively as the chain size is reduced. It is also evident from Figures 4-6 that the major differences in the reduced second virial occur when there are relative few segments in the chain. The reduced second virial coefficient of hard convex body chains with a large number of segments ($m > 30$) appear to approach a common value irrespective of the shape of the HCB segment.

Equation (7) provides a relatively simple means of investigating the properties of hard convex body chains. Ideally it would be useful to compare the predictions with molecular simulation [26]. To the best of our knowledge, molecular simulation data in the literature for hard-body chains are confined exclusively to hard-sphere chains and no simulation data exists for the hard convex body chains examined in this work.

4. Conclusions

A relatively simple equation of state has been developed that is capable of predicting the properties of hard convex body chains. The only two equation of state parameters are related rigorously to the geometry of the hard convex body. The calculation of the compressibility factors and second virial coefficients of hard chains consisting of prolate spherocylinders, oblate spherocylinders and doublecones indicate that these properties are very sensitive to segment shape. The hard convex body equation of state is potentially a useful basis for the development of equations for real molecular chain fluids.

Acknowledgement

I thank Professor Tomáš Boublík for very helpful discussions concerning the site-site correlation function at contact of hard convex bodies.

References

- [1] SADUS, R. J., 1992, *High Pressure Phase Behaviour of Multicomponent Fluid Mixtures* (Amsterdam, Elsevier).
- [2] CARNAHAN, N. F., and STARLING, K. E., 1969, *J. Chem. Phys.*, **51**, 635.
- [3] GUGGENHEIM, E. A., 1965, *Mol. Phys.*, **9**, 43.
- [4] WEI, Y. S., and SADUS, R. J., 1999, *AIChE J.*, submitted.
- [5] CHIEW, Y. C., 1991, *Mol. Phys.*, **73**, 359.
- [6] WERTHEIM, M. S., 1987, *J. Chem. Phys.*, **87**, 7323.
- [7] SONG, Y. and PRAUSNITZ, J. M., 1994, *Macromol.*, **27**, 441.
- [8] CHAPMAN, W. G., GUBBINS, K. E., JACKSON, G. and RADOSZ, M., 1990, *Ind. Eng. Chem. Res.*, **29**, 1709.
- [9] GHONASGI, D., and CHAPMAN, W. G., 1994, *J. Chem. Phys.*, **100**, 6633.
- [10] CHANG, J. and SANDLER, S. I., 1994, *Chem. Eng. Sci.*, **49**, 2777.
- [11] SADUS, R. J., 1995, *J. Phys. Chem.*, **99**, 12363.
- [12] SADUS, R. J., 1996, *Macromol.*, **29**, 7212.
- [13] KIM, C.-H., VIMALCHAND, P., DONOHUE, M. D. and SANDLER, S. I., 1986, *AIChE J.*, **32**, 1726.
- [14] BOUBLÍK, T., 1981, *Ber. Bunsen-Ges. Phys. Chem.*, **85**, 1038.
- [15] KIHARA, T., 1963, *Adv. Chem. Phys.*, **5**, 147.
- [16] SVEJDA, P., and KOHLER, F., 1983, *Ber. Bunsen-Ges. Phys. Chem.*, **87**, 672.
- [17] SADUS, R. J., YOUNG, C. L., and SVEJDA, P., 1988, *Fluid Phase Equilib.*, **39**, 89.
- [18] CHRISTOU, G., SADUS, R. J., YOUNG, C. L., and SVEJDA, P., 1989, *Ind. Eng. Chem. Res.*, **28**, 481.
- [19] CHEN, S. S., and KREGLEWSKI, A., 1977, *Ber. Bunsen-Ges. Phys. Chem.*, **81**, 1048.
- [20] PFOHL, O., and BRUNNER, G., 1998, *Ind. Eng. Chem. Res.*, **37**, 2966.
- [21] CHAPMAN, W. G., JACKSON, G. and GUBBINS, K. E., 1988, *Mol. Phys.*, **65**, 1057.
- [22] BOUBLÍK, T., 1999, personal communication.
- [23] PERCUS, J. K., and YEVICK, G. J., 1958, *Phys. Rev.*, **110**, 1.
- [24] REED, T. M., and GUBBINS, K. E., 1973, *Applied Statistical Mechanics: Thermodynamic and Transport Properties of Fluids* (New York, McGraw-Hill).
- [25] BOUBLÍK, T., and NEZBEDA, I., 1986, *Coll. Czech. Chem. Commun.*, **51**, 2301.
- [26] SADUS, R. J., 1999, *Molecular Simulation of Fluids: Theory, Algorithms and Object-Oriented* (Amsterdam, Elsevier).

Table 1. Geometrical formulae of hard convex body (HCB) shapes studied in this work*.

Shape	R	S	V	α
Sphere	$\sigma/2$	$\pi\sigma^2$	$\frac{\pi\sigma^3}{6}$	1
Prolate spherocylinder	$\frac{(\gamma+1)\sigma}{4}$	$\gamma\pi\sigma^2$	$\frac{(3\gamma-1)\pi\sigma^3}{12}$	$\frac{\gamma^2+\gamma}{3\gamma-1}$
Oblate spherocylinder	$\frac{(0.25\pi(\gamma-1)+1)\sigma}{2}$	$\frac{((\gamma-1)^2+\pi(\gamma-1)+2)\pi\sigma^2}{2}$	$\frac{(6(\gamma-1)^2+3\pi(\gamma-1)+4)\pi\sigma^3}{24}$	$\frac{(0.5\pi(\gamma-1)+1)\sigma}{6(\gamma-1)}$
Doublecone	$\frac{(\gamma+1/\gamma)\sigma}{4}$	$\frac{(\gamma+1/\gamma)\pi\sigma^2}{2}$	$\frac{(\gamma+1/\gamma)\pi\sigma^3}{12}$	$\frac{\gamma+1/\gamma}{2}$

* The symbol σ represents the breadth of the HCB and γ is the maximum length/breadth ratio.

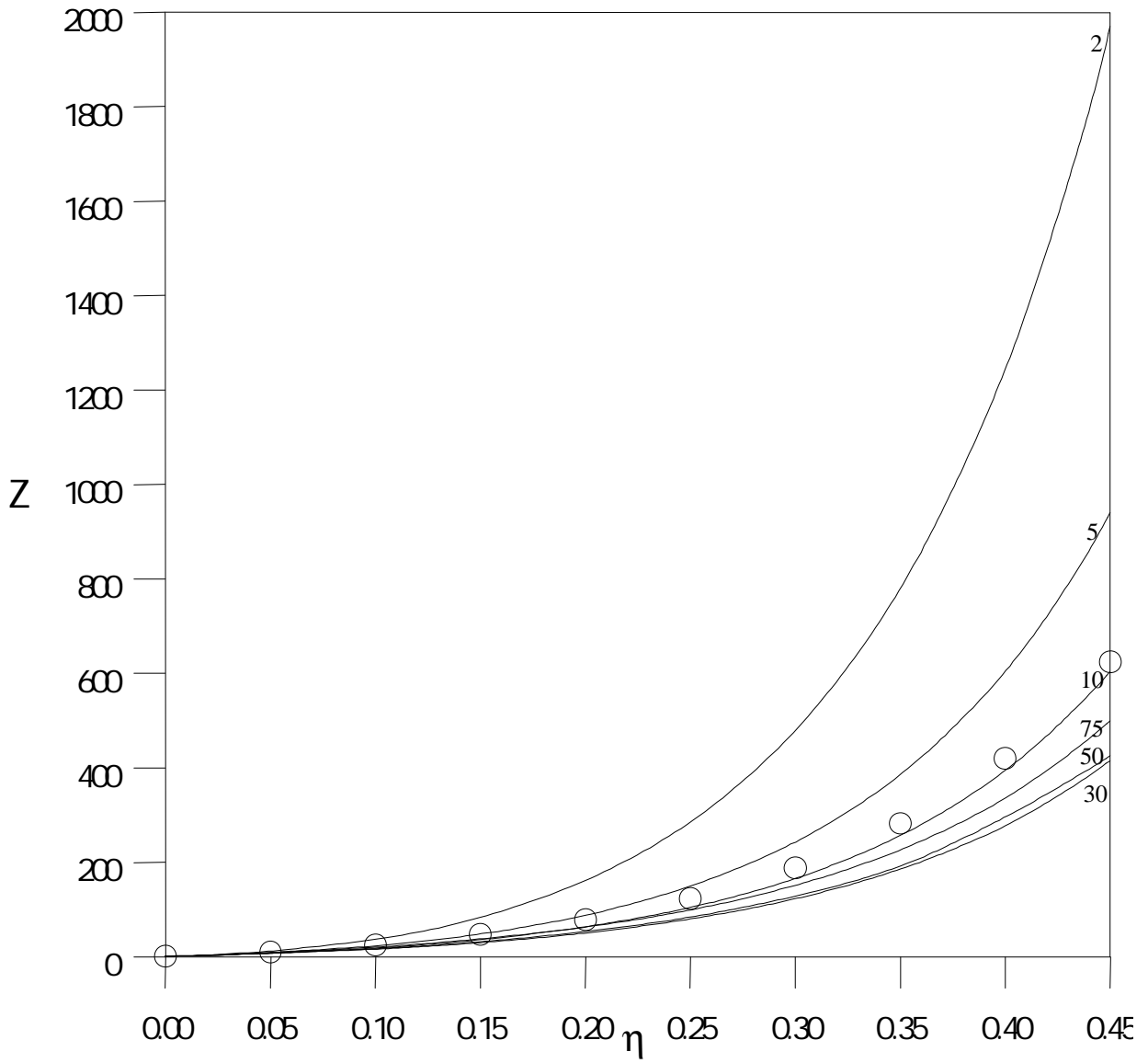


Figure 1. The compressibility factor of various prolate spherocylinder chains ($m = 2, 5, 10, 30, 50, 75$) of length 100σ compared with the compressibility factor of the hard-sphere chain (O).

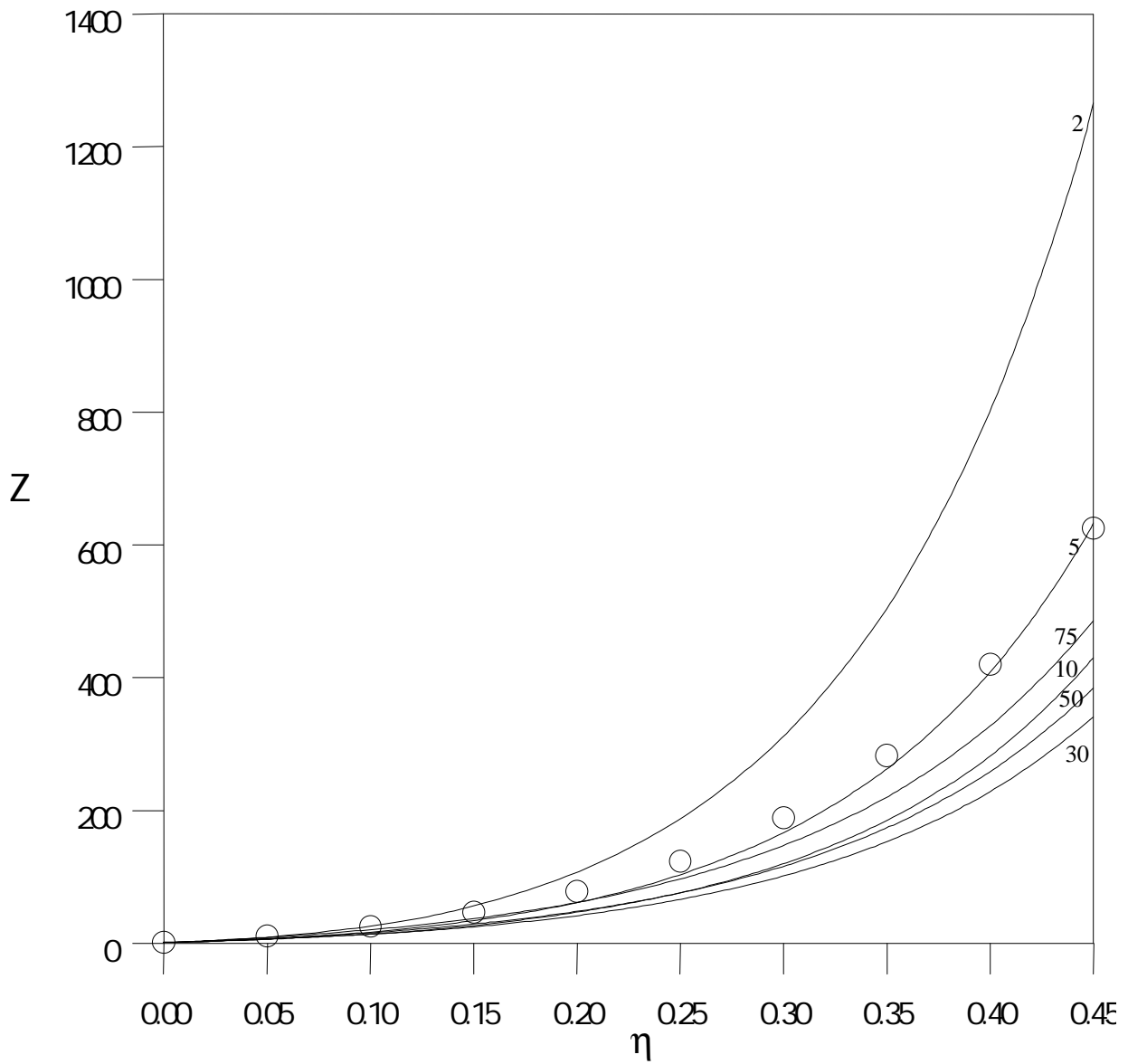


Figure 2. The compressibility factor of various oblate spherocylinder chains ($m = 2, 5, 10, 30, 50, 75$) of length 100σ compared with the compressibility factor of the hard-sphere chain (O).

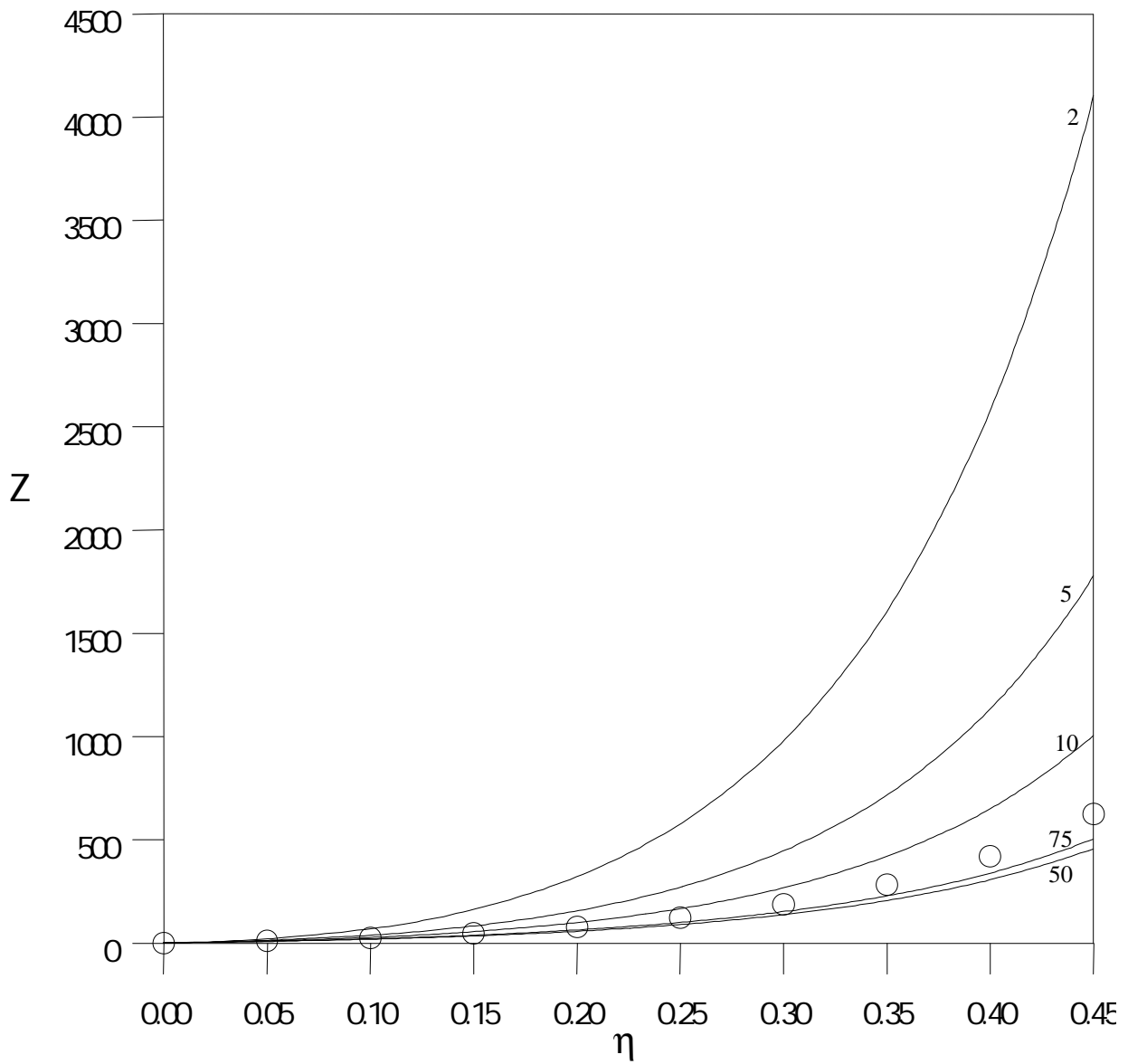


Figure 3. The compressibility factor of various doublecone chains ($m = 2, 5, 10, 30, 50, 75$) of length 100σ compared with the compressibility factor of the hard -sphere chain (O).

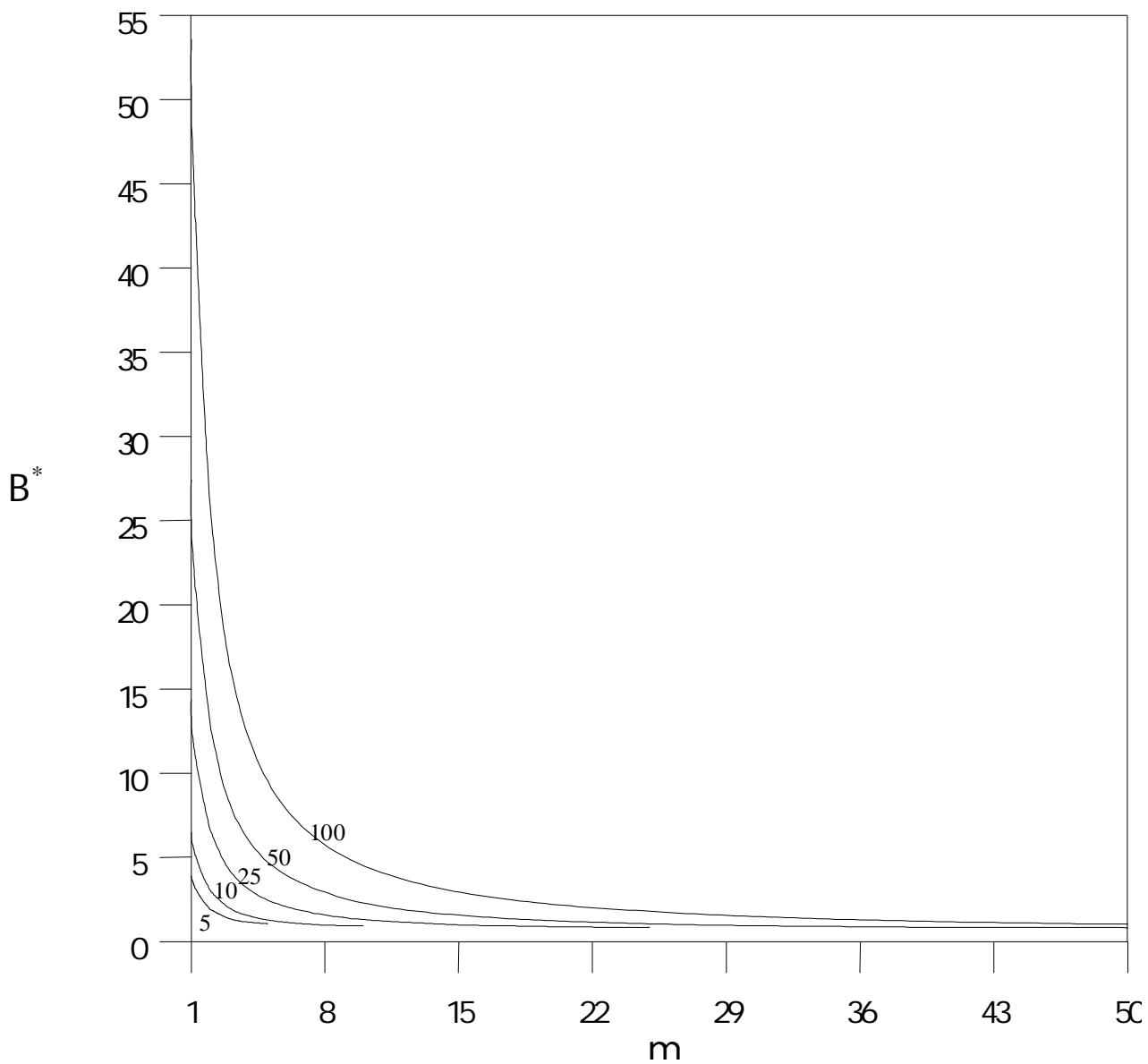


Figure 4. The reduced second virial coefficient of prolate spherocylinder chains of various lengths (5σ , 10σ , 25σ , 50σ , 100σ) as a function of the number of prolate spherocylinder segments.

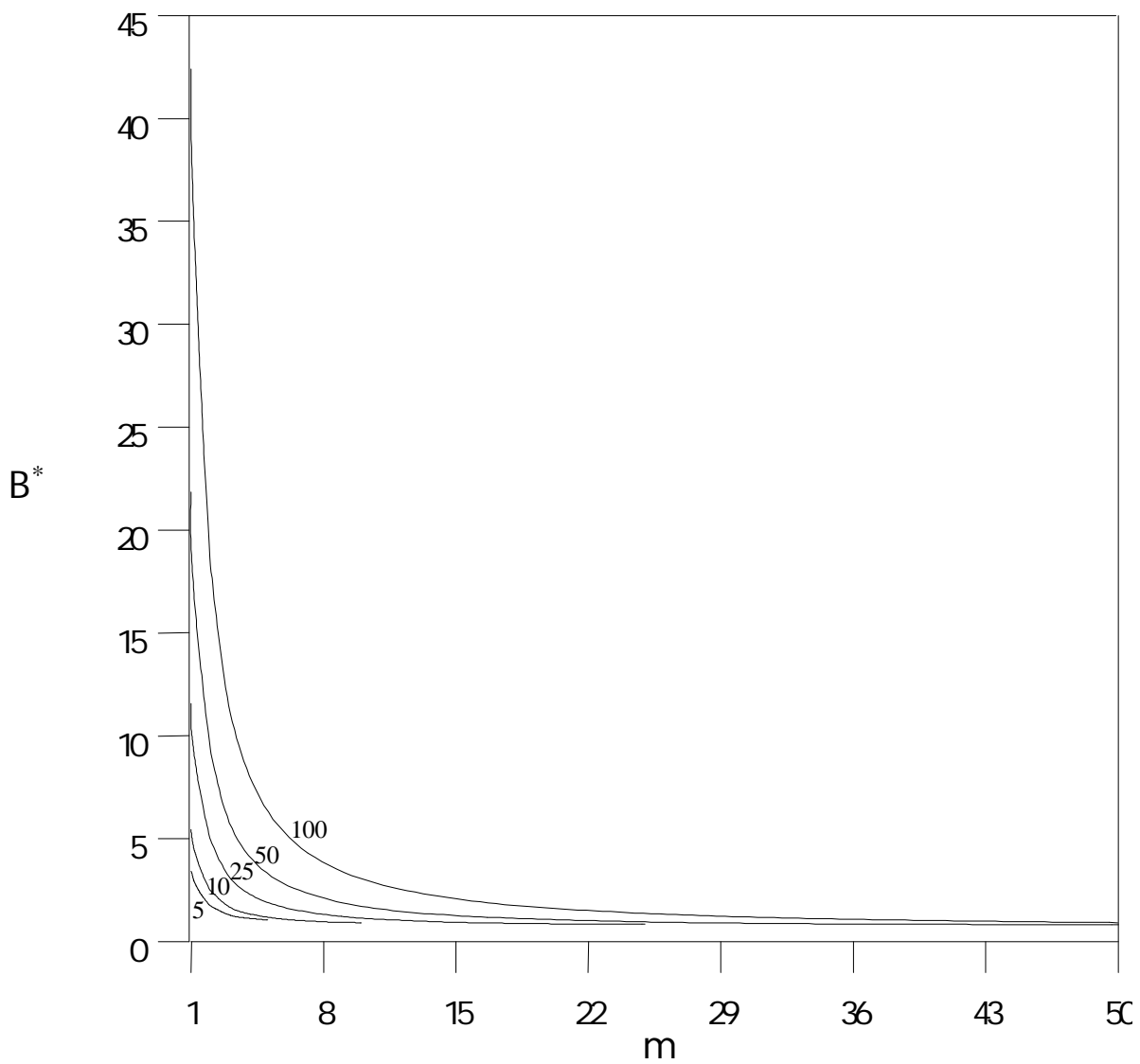


Figure 5. The reduced second virial coefficient of oblate spherocylinder chains of various lengths (5σ , 10σ , 25σ , 50σ , 100σ) as a function of the number of oblate spherocylinder segments.

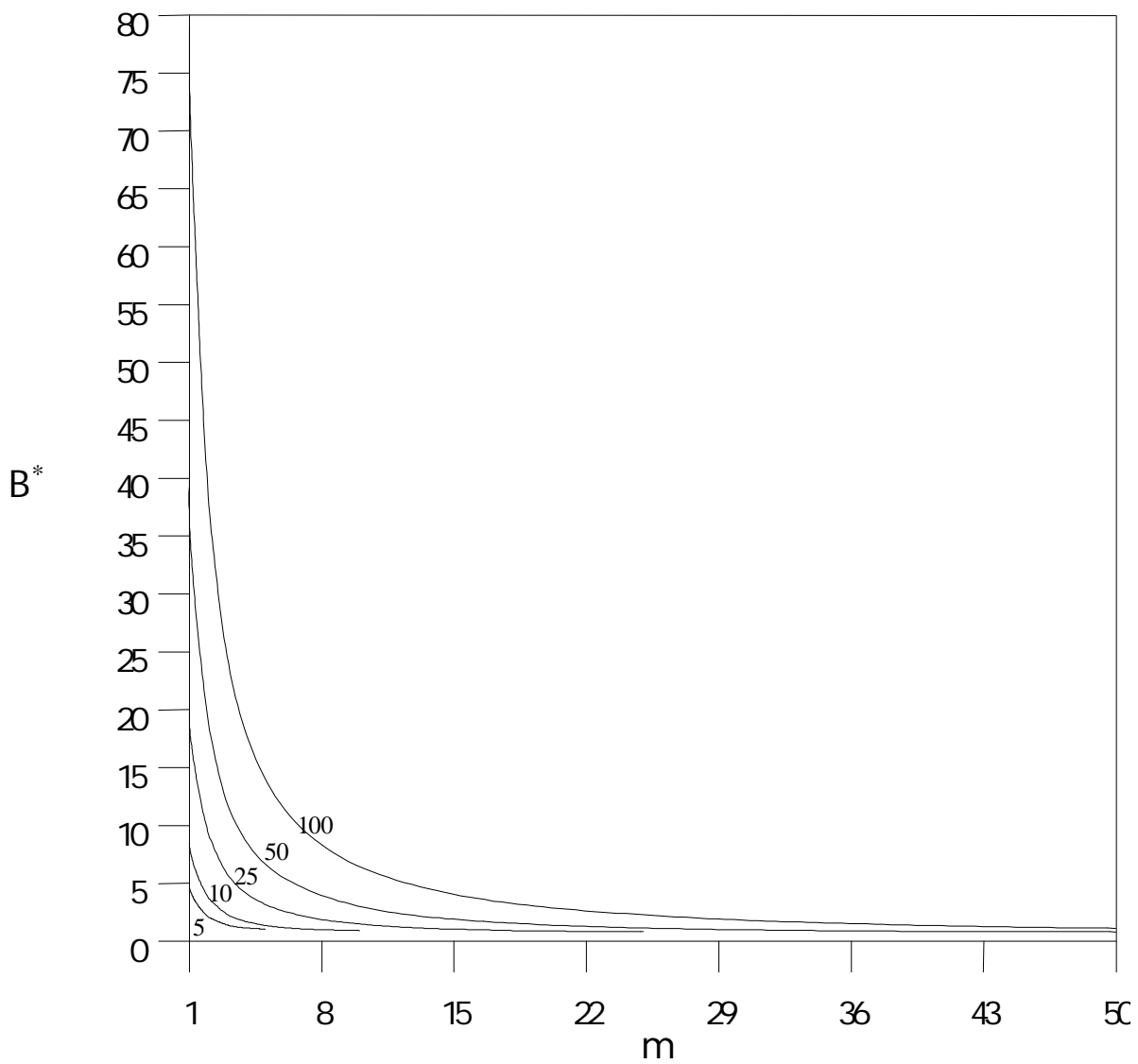


Figure 6. The reduced second virial coefficient of doublecone chains of various lengths (5σ , 10σ , 25σ , 50σ , 100σ) as a function of the number of oblate doublecone segments